Chemical Science

EDGE ARTICLE

View Article Online
View Journal | View Issue

Open Access Article. Published on 28 October 2015. Downloaded on 6/28/2025 11:40:47 AM.
This article is licensed under a Creative Commons Attribution-NonCommercial 3.0 Unported Licence.

CrossMark click for updates

Cite this: *Chem. Sci.*, 2016, **7**, 1051

A highly selective near-infrared fluorescent probe for imaging H_2Se in living cells and *in vivo*†

Fanpeng Kong, Lihong Ge, Xiaohong Pan, Kehua Xu,* Xiaojun Liu and Bo Tang*

Received 15th September 2015
Accepted 28th October 2015

DOI: 10.1039/c5sc03471j

www.rsc.org/chemicalscience

Hydrogen selenide (H_2Se), a highly reactive Se species, is an important selenium metabolism intermediate involved in many physiological and pathological processes. This compound is of scientific interest with regard to the real-time monitoring of H_2Se in living cells and *in vivo* to understand the anti-cancer mechanism of selenium. However, monitoring H_2Se in living cells is still challenging due to the lack of straight forward, highly selective and rapid methods. Here, we developed a novel small-molecule fluorescent probe, **NIR-H_2Se**, for imaging endogenous H_2Se. **NIR-H_2Se** exhibited high selectivity toward H_2Se over selenocysteine (Sec), H_2S and small molecule thiols and was successfully used to image the H_2Se content in HepG2 cells during Na_2SeO_3-induced apoptosis. Increased H_2Se content and reduced ROS levels were observed under hypoxic conditions compared to normoxic conditions, which indicated that the cell apoptosis induced by Na_2SeO_3 under a hypoxic environment is *via* a non-oxidative stress mechanism. Thus, this probe should serve as a powerful tool for exploring the physiological function of H_2Se and Se anticancer mechanisms in a variety of physiological and pathological contexts.

Introduction

Selenium (Se) is an essential trace element for various physiological functions in the human body. Insufficient or excessive Se intake has been associated with a number of diseases.[1,2] Importantly, selenium plays a role in cancer prevention and treatment.[3] However, the anticancer mechanism for Se is still not fully understood. The effectiveness of Se compounds as anticancer agents is correlated to their chemical form and dose.[4] H_2Se, a reduced form of selenium, is an important metabolite of dietary Se compounds.[5] Endogenous H_2Se is generated by reducing selenite *via* GSH and other reduction systems[6] and is involved in many physiological and pathological processes.[7] A reliable and rapid method to determine H_2Se *in vivo* must be developed to investigate the physiological function of H_2Se and the anticancer mechanism of Se.

Fluorescent probes with high sensitivity, good selectivity, and short response times *via* direct observation are powerful tools for the *in vivo* detection of biomolecules.[8] Several fluorescent probes for detecting Se species were recently reported. Maeda *et al.* developed the first fluorescent probe, BESThio, to discriminate selenols from their Cys counterparts based on their different nucleophilicity at pH = 5.8.[9] Using the recognition group Maeda reported, Fang and Lin exploited probes by adjusting the fluorophore to detect selenols with high selectivity under physiological conditions.[10] In addition, Fang *et al.* developed another novel fluorescent probe (TRFS-green) using a 1,2-dithiolane reporter group to selectively image thioredoxin reductase (TrxR) at pH = 7.4.[11] Wu reported a cadmium sulfide (CdS) quantum dot (QD) probe for HSe^- ions in aqueous solution.[12] However, a small-molecule fluorescent probe for imaging the highly reactive H_2Se in living cells and *in vivo* has not been reported.

Previously, our group discovered that the Se–N bond can be cleaved using sulfhydryl groups and we developed a series of fluorescence methods to monitor thiols and their redox state in living cells.[13–15] We subsequently found that the Se–N bond in 2,1,3-benzoselenadiazole (BS) can be specifically broken by selenol *via* direct nucleophilic addition and we designed a new fluorescent probe (HB) to image endogenous Sec in living cells and *in vivo*.[16] These results inspired us to develop a H_2Se fluorescent probe based on the BS group by modifying the probe molecule structure.

Here, we integrated the BS moiety into a near infrared (NIR) merocyanine dye[17] to develop a novel small-molecule fluorescent probe for detecting H_2Se (**NIR-H_2Se**). **NIR-H_2Se** responds to H_2Se rapidly, with a high selectivity over H_2S, Sec and biological thiols and was used to successfully image endogenous H_2Se in living cells and *in vivo*. Moreover, we used a radical oxygen species (ROS) probe and found that the H_2Se contents increased during HepG2 cell apoptosis induced by Na_2SeO_3 in a time- and

College of Chemistry, Chemical Engineering and Materials Science, Collaborative Innovation Center of Functionalized Probes for Chemical Imaging in Universities of Shandong, Key Laboratory of Molecular and Nano Probes, Ministry of Education, Shandong Provincial Key Laboratory of Clean Production of Fine Chemicals, Shandong Normal University, Jinan 250014, P. R. China. E-mail: tangb@sdnu.edu.cn; xukehua@sdnu.edu.cn

† Electronic supplementary information (ESI) available: The NMR and HR MS spectra of **NIR-H_2Se**, HPLC analysis of the reaction of the probe and H_2Se, and other materials. See DOI: 10.1039/c5sc03471j

Open Access Article. Published on 28 October 2015. Downloaded on 6/28/2025 11:40:47 AM.
This article is licensed under a Creative Commons Attribution-NonCommercial 3.0 Unported Licence.

dose-dependent manner, while the ROS level did not change under a hypoxic environment. This probe will provide a powerful tool for investigating the metabolism and antitumor mechanism of Se compounds.

Results and discussion

The syntheses are illustrated in Scheme 1, and the probe and intermediate structures were fully characterized by ^{1}H NMR, ^{13}C NMR, and HRMS. We first examined the spectroscopic properties of this probe and optimized the fluorescence measurement conditions (Fig. S1 and S2, ESI†). **NIR-H_2Se** exhibits an emission maximum at 735 nm with weak fluorescence (Φ = 0.019) in aqueous solutions buffered at physiological pH (10 mM phosphate buffered saline, PBS, pH = 7.4) due to effective fluorescence quenching of the BS *via* the heavy atom effect of Se. As predicted, the BS moiety in **NIR-H_2Se** reacts selectively with H_2Se over Sec, H_2S, and small molecule thiols. The HPLC analysis confirmed that the fluorescent product was a diamino product (Scheme 2 and Fig. S3 and S4, ESI†).

We then tested the fluorescence response to H_2Se. Adding H_2Se increased the fluorescence intensity of **NIR-H_2Se** *ca.*10-fold (Φ = 0.13, Fig. 1a). There was good linearity between the fluorescence intensities and H_2Se concentrations for the range 0–12 μM (Fig. 1b). The regression equation was F = 2096.7 + 1772.3[H_2Se] μM with a linear coefficient of 0.9941. The limit of detection was 7.0 nM (standard deviation 3.5%, n = 11).

To evaluate the selectivity of **NIR-H_2Se** for H_2Se, we measured the fluorescence spectra for the probe with H_2Se, H_2S and thiols. High concentrations of thiols such as cysteine (Cys), homocysteine (Hcy) and glutathione (GSH) (1 mM for each) produced low fluorescence responses, and **NIR-H_2Se** also gave a negative response for H_2S, Sec, Na_2SeO_3, *N*-acetyl-L-cysteine (NAC), thioredoxin reductase (TrxR) and vitamin C (Vc). The reactivity of **NIR-H_2Se** towards ROS was then tested. Fig. 2a shows that biologically relevant ROS, including H_2O_2, $^{-}$OCl, $O_2^{\bullet -}$, and ROO$^{\bullet}$, did not trigger any fluorescence changes in the probe. Moreover, considering that nitric oxide (NO) may be a potential interfering species,[18] the fluorescence response of **NIR-H_2Se** to differing amounts of NO were studied both with and without H_2Se. The results indicated that even high NO concentrations (10 equiv.) did not induce an obvious fluorescence change in the detection system. The interference from

Scheme 2 Proposed mechanism for the selective reaction of H_2Se.

metal ions and other amino acids were also tested as shown in Fig. S5 and S6.† Collectively, **NIR-H_2Se** selectively recognized H_2Se under physiological conditions.

Considering the variable nature and quick metabolism of endogenous H_2Se in biological systems, a fast-responding method for H_2Se detection is necessary. The response of **NIR-H_2Se** to H_2Se was evaluated *via* a kinetics experiment. The results indicated that the fluorescence intensity immediately increased to its maximum after adding H_2Se to the probe solution, which indicated that the probe instantly responds to H_2Se (Fig. 2b). In addition, the cytotoxicity of the probe in HepG2 cells was determined *via* a conventional MTT assay (Fig. S7, ESI†), which indicated that the **NIR-H_2Se** probe exhibited low biotoxicity and could be used as a viable probe for detecting H_2Se in biological samples.

After confirming the high sensitivity, selectivity and rapid response of this probe for H_2Se, we explored its applications to image endogenous H_2Se in living cells. During these cell imaging experiments, Na_2SeO_3 was used as the H_2Se precursor because sodium selenite can be metabolized to hydrogen selenide (H_2Se) *via* selenodiglutathione (GSSeSG) and glutathione selenenylsulfide (GSSeH).[19] HepG2 cells were treated with 2–10 μM Na_2SeO_3 for 12 h or incubated with 5 μM Na_2SeO_3 for 2–12 h, as our previous study found that these action concentrations and times of Na_2SeO_3 can induce HepG2 cell apoptosis.[16] After treatment, the cells were loaded with 10 μM of **NIR-H_2Se**. The experimental results are shown in Fig. 3. Higher H_2Se contents were observed in hypoxic environments than under normoxic conditions during these parallel experiments.

We found that the apparent discrepancies above were related to the aerobic metabolism of H_2Se. Under normoxic conditions (20% pO_2), H_2Se rapidly oxidized to generate a mass of superoxide anion radicals ($O_2^{\bullet -}$) and an accumulation of reactive

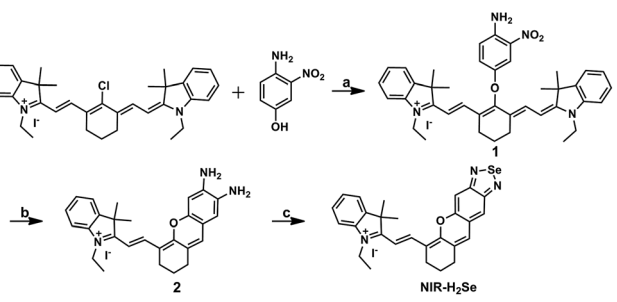

Scheme 1 Synthesis of NIR-H_2Se. Reaction conditions: (a) NaH, DMF, rt, 73%; (b) $SnCl_2$, HCl, CH_3OH, 70 °C, 45%; (c) SeO_2, grind, 71%.

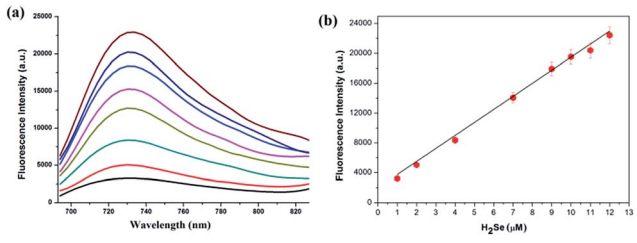

Fig. 1 (a) Fluorescence response of 10 μM NIR-H_2Se to differing amounts of H_2Se. (b) Linear correlation between the emission intensity and H_2Se concentration. All spectra were acquired in 10 mM PBS with a pH of 7.4 ($\lambda_{ex}/\lambda_{em}$ = 688/735 nm). The data were expressed as the mean ± standard deviation (SD) across three experiments.

This journal is © The Royal Society of Chemistry 2016

Open Access Article. Published on 28 October 2015. Downloaded on 6/28/2025 11:40:47 AM.
This article is licensed under a Creative Commons Attribution-NonCommercial 3.0 Unported Licence.

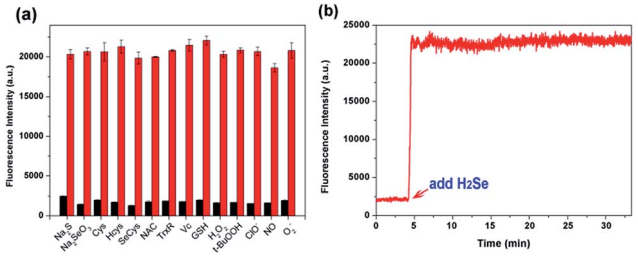

Fig. 2 (a) Fluorescence intensity changes for **NIR-H_2Se** (10 μM) after adding 100 equiv. of thiols, Na_2S, Na_2SeO_3, Sec, NAC, TrxR, Vc, various biologically related ROS and 10 equiv. of NO. The black bars show the addition of one of these interferents to a 10 μM **NIR-H_2Se** solution. The red bars represent the addition of both H_2Se and one interferent to the probe solution. (b) Time course for the fluorescence intensity of 10 μM **NIR-H_2Se** with 10 μM H_2Se in a 10 mM PBS, pH = 7.4, at room temperature.

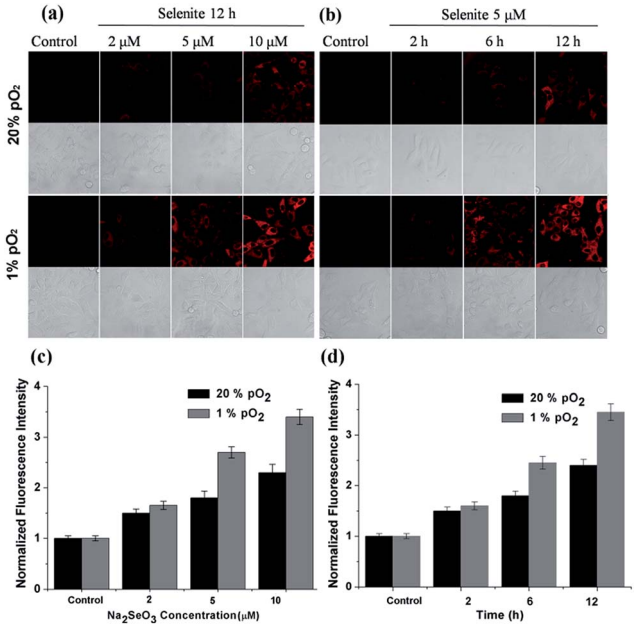

Fig. 3 Confocal fluorescence imaging of endogenous H_2Se in HepG2 cells treated with sodium selenite under normoxic (20% pO_2) and hypoxic (1% pO_2) conditions. (a) The fluorescence changes for the HepG2 cells exposed to different sodium selenite concentrations (2–10 μM) for 12 h and incubated with **NIR-H_2Se** (10 μM). (b) The fluorescence changes of the HepG2 cells exposed to 5 μM of sodium selenite for different times (0–12 h) and incubated with **NIR-H_2Se** (10 μM). The fluorescence was imaged using a confocal microscope with 633 nm excitation and 650–750 nm collection. (c) The fluorescence intensity for (a). (d) The fluorescence intensity for (b). The data were normalized to the control, and statistical analyses were performed using a two-tailed Student's *t*-test ($n \geq 4$ fields of cells) relative to the control. *$P < 0.01$ and the error bars are ± the standard error measurement.

oxygen species during the tumor apoptosis process induced by Na_2SeO_3.[20] However, under a hypoxic environment (1% pO_2), H_2Se cannot quickly metabolize due to the lack of oxygen, which allows H_2Se to effectively accumulate. To further confirm our viewpoint, the H_2O_2 content was evaluated using a H_2O_2 probe[21] for parallel experiments.

HepG2 cells were treated with different Na_2SeO_3 concentrations for 12 h or incubated with 5 μM Na_2SeO_3 for differing times before loading with 10 μM of the H_2O_2 probe. Fig. 4 shows that the H_2O_2 content gradually increased under normoxic conditions in the HepG2 cells with Na_2SeO_3 in a time- and dose-dependent manner, while low H_2O_2 levels were maintained under hypoxic conditions during the parallel experiments. These results indicate that the Na_2SeO_3 anticancer mechanism is not a ROS-induced apoptosis process under hypoxic conditions. Because hypoxia is a characteristic feature of solid tumors due to the imbalance between new blood vessel formation and rapid cancer cell proliferation,[22] these results also imply that the anticancer effect of Na_2SeO_3 in solid tumors is not owed to oxidative stress.[23]

The above results indicate that **NIR-H_2Se** has potential for detecting endogenous H_2Se *in vivo*. To evaluate this proposal, mice bearing subcutaneously implanted tumors grown from murine hepatoma cell line H22 were subcutaneously injected with buffer solutions containing **NIR-H_2Se** (10 μM) and sodium selenite (10 μM), and fluorescence images were then obtained at

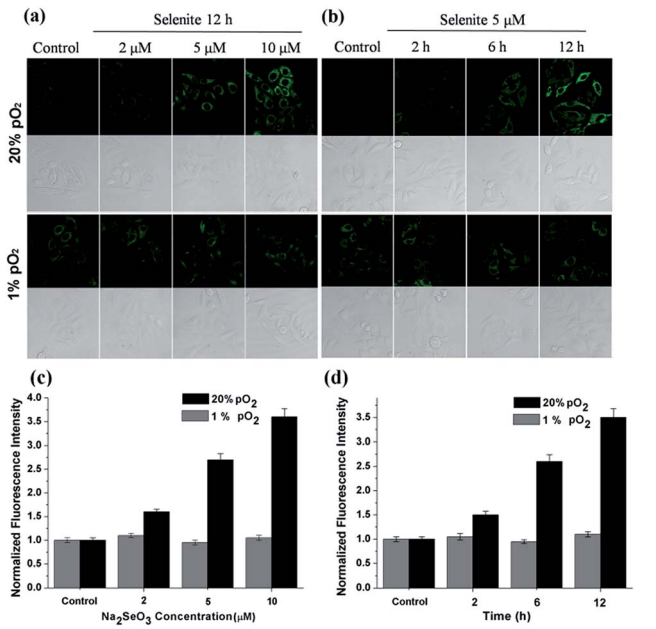

Fig. 4 Confocal fluorescence imaging of H_2O_2 in HepG2 cells treated with sodium selenite under normoxic (20% pO_2) and hypoxic (1% pO_2) environments. (a) The fluorescence changes in the HepG2 cells exposed to different sodium selenite concentrations (2–10 μM) for 12 h and incubated with a H_2O_2 probe (10 μM). (b) The fluorescence changes for the HepG2 cells exposed to a 5 μM sodium selenite solution for different times (0–12 h) and incubated with a H_2O_2 probe (10 μM). The fluorescence was imaged using a confocal microscope with 532 nm excitation and 600–700 nm collection. (c) The fluorescence intensity for (a). (d) The fluorescence intensity for (b). The data were normalized to the control, and statistical analyses were performed using a two-tailed Student's *t*-test ($n \geq 4$ fields of cells) relative to the control. *$P < 0.01$ and the error bars are ± the standard error measurement.

Open Access Article. Published on 28 October 2015. Downloaded on 6/28/2025 11:40:47 AM.
This article is licensed under a Creative Commons Attribution-NonCommercial 3.0 Unported Licence.

different times using an *in vivo* imaging system (IVIS). Fig. 5 shows that the fluorescence signal of the probe was exclusively observed in the tumor region without a background signal, and that the fluorescence intensity increased from 3 h to 12 h post injection. The results indicated that the hypoxic solid tumor generated H_2Se from sodium selenite and that the H_2Se gradually accumulated.

Conclusions

In summary, we developed a novel small-molecule fluorescent probe, **NIR-H_2Se**, to detect H_2Se. The probe rapidly responded to H_2Se, exhibited high sensitivity and good selectivity for H_2Se over Sec, H_2S, ROS and other sulfur-containing species and was successfully used to image endogenous H_2Se in living cells and *in vivo*. Furthermore, we found that normoxic conditions increased the H_2O_2 content, while the H_2Se level rose only slightly during HepG2 cell apoptosis induced by Na_2SeO_3. However, H_2Se accumulated gradually and the ROS remained low in a hypoxic environment. These findings indicate that the anticancer mechanism of Se for hypoxic solid tumors is *via* non-oxidative stress. We anticipate that the current probe will provide an ideal tool for further studies into the biological functions of H_2Se and Se anticancer mechanisms.

Experimental

Materials and instruments

All chemicals were available commercially and the solvents were purified by conventional methods before use. Cysteine (Cys), homocysteine (Hcy), glutathione (GSH) and 3-(4,5-dimethylthiazol-2yl)-2,5-diphenyltetrazolium bromide (MTT) were purchased from Sigma Chemical Company. Na_2SeO_3, *N*-acetyl-L-cysteine (NAC), thioredoxin reductase (TrxR) and vitamin C (Vc) were purchased from Sigma-Aldrich Co. Ltd. The silica gel (100–200 mesh) was used for the flash chromatography. Cy.7.Cl was synthesized in our laboratory. Sartorius ultrapure water (18.2 MΩ cm) was used throughout the analytical experiments. H_2Se was prepared by the reaction of Al_2Se_3 with H_2O in an N_2 atmosphere for 30 min at room temperature before use every time.[24] H_2O_2, *tert*-butylhydroperoxide (TBHP), and hypochlorite (NaOCl) were delivered from 30%, 70%, and 10% aqueous solutions respectively. Nitric oxide (NO) was used from a stock solution prepared by sodium nitroprusside. Superoxide ($O_2^{\bullet-}$) was delivered from KO_2 in DMSO solution or from xanthine oxidase.

^1H NMR and ^{13}C NMR spectra were determined using 300 MHz and 400 MHz Bruker NMR spectrometers. The mass spectra were obtained using a Bruker maXis ultra-high resolution-TOF MS system. The melting points were measured using a SGW X-4 Melting Point Tester. The fluorescence spectra measurements were performed using an FLS-920 Fluorescence Spectrometer (Edinburgh Instruments, UK). All pH measurements were performed with a pH-3c digital pH-meter (Shanghai Lei Ci Device Works, Shanghai, China) with a combined glass/calomel electrode. The fluorescence images of cells were taken using a TCS SP5 confocal laser scanning microscope with an objective lens (×40). The absorbance was measured using a TRITURUS microplate reader in the MTT assay.

Synthesis and characterization of NIR-H_2Se

Synthesis of compound 1. 4-Amino-3-nitrophenol (39 mg, 0.25 mmol) and NaH (60% in mineral oil) (10 mg, 0.25 mmol) were dissolved in anhydrous *N*,*N*-dimethylformamide (DMF) (7 mL). The mixture was stirred at room temperature for 10 min under an argon atmosphere. Then a solution of heptamethine cyanine chlorine (Cy.7.Cl) (64 mg, 0.10 mmol) in anhydrous DMF (2 mL) was added to the mixture *via* a syringe. The reaction mixture was further stirred for 4 h at room temperature. The solvent was removed under reduced pressure, then the crude product was purified by silica gel chromatography with 6% MeOH in dichloromethane (DCM) to afford the desired product as a dark green solid (55 mg, 73%). mp = 149–150 °C. ^1H NMR (400 MHz, $CDCl_3$): δ 1.26–1.40 (m, 18H), 2.03 (s, 4H), 2.17 (s, 2H), 2.68 (s, 4H), 4.08 (s, 4H), 5.97 (d, J = 12 Hz, 2H), 7.09 (d, J = 8 Hz, 2H), 7.21–7.29 (m, 5H), 7.54 (s, 3H), 7.80 (d, J = 8 Hz, 1H), 7.92 (d, J = 12 Hz, 2H). ^{13}C NMR (75 MHz, $CDCl_3$): δ 12.2, 21.0, 24.3, 27.8, 39.4, 49.1, 99.3, 108.3, 110.2, 122.1, 122.4, 125.3, 128.7, 141.1, 141.5, 142.2, 143.4, 164.4, 171.7. HR MS $[M - I]^+$: m/z calcd 629.3486, found 629.3455.

Synthesis of compound 2. $SnCl_2$ (900 mg, 4 mmol) and concentrated HCl (0.8 mL) were added to a solution of compound **1** (151 mg, 0.20 mmol) in MeOH (6 mL), stirred, and maintained at 70 °C overnight under an argon atmosphere. The mixture was neutralized with 2 N NaOH, and the precipitate was removed by filtration and washed with DCM. The filtrate and washings were washed with water. The organic layer was dried over Na_2SO_4, and the solvent was evaporated to yield a dark green solid (49 mg, 45%). mp = 225–228 °C. ^1H NMR (400 MHz, $CDCl_3$): δ 1.31 (s, 3H), 1.69 (s, 6H), 1.84 (s, 2H), 2.57 (s, 2H), 2.70 (s, 2H), 3.89 (s, 2H), 4.63 (s, 1H), 5.68 (s, 1H), 6.75 (s, 1H), 6.86–6.92 (m, 2H), 7.03 (s, 1H), 7.28 (s, 2H), 7.39 (s, 2H), 8.10 (d, J = 12 Hz, 1H). ^{13}C NMR (75 MHz, $CDCl_3$): δ 11.6, 21.0, 24.5, 28.3, 28.7, 48.0, 97.5, 107.2, 108.4, 115.7, 121.5, 128.2, 137.1, 139.3, 148.5, 152.6, 160.8, 166.8. HR MS $[M - I]^+$: m/z calcd 412.2383, found 412.2378.

Synthesis of NIR-H_2Se. To a porcelain mortar was added compound **2** (108 mg, 0.20 mmol) and SeO_2 (22 mg, 0.2 mmol).

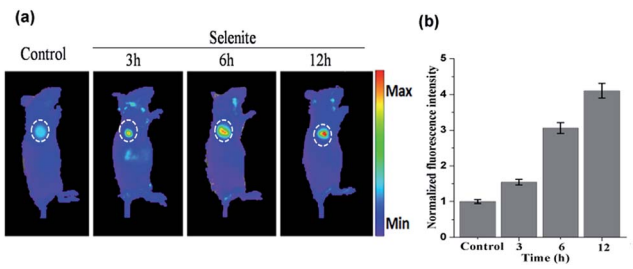

Fig. 5 (a) *In vivo* fluorescence imaging of H22 tumor-bearing mice injected with the probe NIR-H_2Se (10 μM) in response to sodium selenite (10 μM) at different times. (b) The fluorescence intensity for (a). The data were normalized to the control.

This journal is © The Royal Society of Chemistry 2016

Open Access Article. Published on 28 October 2015. Downloaded on 6/28/2025 11:40:47 AM. This article is licensed under a Creative Commons Attribution-NonCommercial 3.0 Unported Licence.

The mixture was fully grinded for 30 min, and TLC showed full conversion of compound **2** to the probe. The resulting mixture was extracted by MeOH (20 mL) and the solvent was removed under reduced pressure, then the crude product was purified by silica gel chromatography with 6% MeOH in DCM to afford the desired product as a dark purple solid (87 mg, 71%). mp = 252–253 °C. ^{1}H NMR (400 MHz, $CDCl_3$): δ 1.61 (t, J = 6 Hz, 3H), 1.86 (s, 6H), 2.01 (t, J = 3 Hz, 2H), 2.41 (s, 2H), 2.75 (t, J = 3 Hz, 2H), 3.00 (t, J = 3 Hz, 2H), 5.00 (q, J = 6 Hz, 2H), 7.38 (d, J = 16 Hz, 1H), 7.49 (s, 1H), 7.54–7.59 (m, 4H), 7.68 (s, 1H), 7.74 (d, J = 16 Hz, 1H). ^{13}C NMR (75 MHz, $CDCl_3$): δ 13.7, 14.1, 20.6, 24.5, 29.3, 30.9, 42.9, 51.7, 104.7, 110.7, 114.3, 119.0, 119.6, 122.5, 124.7, 126.5, 128.0, 128.8, 129.7, 132.6, 140.7, 142.9, 146.6, 152.7, 155.5, 179.6. HR MS: $[M - I]^+$: m/z calcd 488.1218, found 488.1237.

Fluorescence analysis

Fluorescence spectra were obtained with an FLS-920 Fluorescence Spectrometer (Edinburgh Instruments, UK). After dilution to 10 μM of the probe with 10 mM PBS, various amounts of H_2Se were added. The fluorescence intensity was measured at $\lambda_{ex}/\lambda_{em}$ = 688/735 nm.

Cell culture

HepG2 cells were maintained following the protocols provided by the American Type Tissue Culture Collection. Cells were first grown in a circular Petri dish (60 mm) using high glucose Dulbecco's Modified Eagle Medium (DMEM, 4.5 g of glucose per L) supplemented with 10% fetal bovine serum (FBS), $NaHCO_3$ (2 g L^{-1}) and 1% antibiotics (penicillin/streptomycin, 100 U mL^{-1}). Cultures were maintained in a humidified incubator at 37 °C, in 5% CO_2/95% air. One day before imaging, cells were passed and plated on 18 mm glass coverslips in a culture dish. The culture medium was refreshed every 24 h. All cells used were in the exponential growth phase.

Confocal imaging

Fluorescence imaging studies were performed with a TCS SP5 confocal laser scanning microscope (Germany Leica Co., Ltd) with an objective lens (×40). Excitation of the H_2Se probe-loaded cells at 633 nm was carried out with an argon laser, and emission was collected using a META detector between 650 and 750 nm. Excitation of the H_2O_2 probe-loaded cells at 532 nm was carried out with an argon laser, and emission was collected using a META detector between 650 and 750 nm. Prior to imaging, the medium was removed. Cell imaging was carried out after washing cells with PBS (pH = 7.4, 10 mM) three times.

Animal and tumor models

All animal experiments were carried out according to the Principles of Laboratory Animal Care (People's Republic of China) and the Guidelines of the Animal Investigation Committee, and approved by the local Animal Care and Use Committee. Six- to eight-week-old female Kunmin male mice were purchased from the Shanghai SLAC Laboratory Animal Co., Ltd. During procedures, the mice were anesthetized with inhaled isoflurane. 1×10^6 H22 cells were injected into the enterocoelia of each Kunmin mouse, ascites were formed after 5 or 7 days, which were further used after three passages. Four- to six-week-old nude mice received a subcutaneous injection of 1×10^6 H22 ascite tumor cells into the axillary lateral subcutaneous of their right forelimbs. Tumors were then allowed to grow over a period of 15 to 20 days until reaching 0.5–1.5 cm in diameter.

Acknowledgements

This work was supported by 973 Program (2013CB933800), National Natural Science Foundation of China (21535004, 21227005, 21390411, 21275092, 21575081 and 21405098).

Notes and references

1 (*a*) C. M. Weekley and H. H. Harris, *Chem. Soc. Rev.*, 2013, **42**, 8870–8894; (*b*) M. P. Rayman, *Lancet*, 2012, **379**, 1256–1268.
2 (*a*) M. A. Reeves and P. R. Hoffmann, *Cell. Mol. Life Sci.*, 2009, **66**, 2457–2478; (*b*) S. Misra, D. Peak, N. Chen, C. Hamilton and S. Niyogi, *Comp. Biochem. Physiol., Part C: Pharmacol., Toxicol. Endocrinol.*, 2012, **155**, 560–565; (*c*) S. J. Fairweather-Tait, Y. Bao, M. R. Broadley, R. Collings, D. Ford, J. E. Hesketh and R. Hurst, *Antioxid. Redox Signaling*, 2011, **14**, 1337–1383.
3 (*a*) C. M. Weekley, J. B. Aitken, S. Vogt, L. A. Finney, D. J. Paterson, M. D. de Jonge, D. L. Howard, I. F. Musgrave and H. H. Harris, *Biochemistry*, 2011, **50**, 1641–1650; (*b*) A. J. Duffield-Lillico, M. E. Reid, B. W. Turnbull, G. F. Combs Jr, E. H. Slate, L. A. Fischbach, J. R. Marshall and L. C. Clark, *Cancer Epidemiol., Biomarkers Prev.*, 2002, **11**, 630–639; (*c*) C. M. Weekley, J. B. Aitken, S. Vogt, L. A. Finney, D. J. Paterson, M. D. de Jonge, D. L. Howard, P. K. Witting, I. F. Musgrave and H. H. Harris, *J. Am. Chem. Soc.*, 2011, **133**, 18272–18279.
4 (*a*) C. M. Weekley and H. H. Harris, *Chem. Soc. Rev.*, 2013, **42**, 8870–8894; (*b*) L. C. Clark, G. F. Combs, B. W. Turnbull, E. H. Slate, D. K. Chalker, J. Chow, L. S. Davis, R. A. Glover, G. F. Graham and E. G. Gross, *J. Am. Med. Assoc.*, 1996, **276**, 1957–1963; (*c*) S. M. Lipp-man, E. A. Klein, P. J. Goodman, M. S. Lucia, I. M. Thompson, L. G. Ford, H. L. Parnes, L. M. Minasian, J. M. Gaziano and J. A. Hartline, *J. Am. Med. Assoc.*, 2009, **301**, 39–51.
5 G. Combs and W. Gray, *Pharmacol. Ther.*, 1998, **79**, 179–192.
6 M. Wallenberg, E. Olm, C. Hebert, M. Björnstedt and A. P. Fer-nandes, *Biochem. J.*, 2010, **429**, 85–93.
7 (*a*) Z. Veres, L. Tsai, T. D. Scholz, M. Politino, R. S. Balaban and T. C. Stadtman, *Proc. Natl. Acad. Sci. U. S. A.*, 1992, **89**, 2975–2979; (*b*) R. S. Glass, W. P. Singh, W. Jung, Z. Veres, T. D. Scholz and T. C. Stadtman, *Biochemistry*, 1993, **32**, 12555–12559; (*c*) Y. Kobayashi, Y. Ogra, K. Ishiwata, H. Takayama, N. Aimi and K. T. Suzuki, *Proc. Natl. Acad. Sci. U. S. A.*, 2002, **99**, 15932–15936.
8 (*a*) L. Yuan, W. Y. Lin, K. B. Zheng, L. W. He and W. M. Huang, *Chem. Soc. Rev.*, 2013, **42**, 622–661; (*b*)

Open Access Article. Published on 28 October 2015. Downloaded on 6/28/2025 11:40:47 AM.
This article is licensed under a Creative Commons Attribution-NonCommercial 3.0 Unported Licence.

Z. Q. Guo, S. Park, J. Y. Yoon and I. Shin, *Chem. Soc. Rev.*, 2014, **43**, 16–29; (*c*) R. Weissleder and V. Ntziachristos, *Nat. Med.*, 2003, **9**, 123–128.

9 H. Maeda, K. Katayama, H. Matsuno and T. Uno, *Angew. Chem., Int. Ed.*, 2006, **45**, 1810–1813.

10 (*a*) B. Zhang, C. Ge, J. Yao, Y. Liu, H. Xie and J. Fang, *J. Am. Chem. Soc.*, 2015, **137**, 757; (*b*) H. Chen, B. Dong, Y. Tang and W. Lin, *Chem.–Eur. J.*, 2015, **21**, 11696–11700.

11 L. Zhang, D. Duan, Y. Liu, C. Ge, X. Cui, J. Sun and J. Fang, *J. Am. Chem. Soc.*, 2014, **136**, 226–233.

12 C. L. Wu and Y. B. Zhao, *Anal. Bioanal. Chem.*, 2007, **388**, 717–722.

13 B. Tang, Y. Xing, P. Li, N. Zhang, F. Yu and G. Yang, *J. Am. Chem. Soc.*, 2007, **129**, 11666–11667.

14 K. Xu, M. Qiang, W. Gao, R. Su, N. Li, Y. Gao, Y. Xie, F. Kong and B. Tang, *Chem. Sci.*, 2013, **4**, 1079–1086.

15 B. Tang, L. Yin, X. Wang, Z. Chen, L. Tong and K. Xu, *Chem. Commun.*, 2009, **45**, 5293–5295.

16 F. Kong, B. Hu, Y. Gao, X. H. Pan, F. Huang, Q. Zheng, H. Chen and B. Tang, *Chem. Commun.*, 2015, **51**, 3102–3105.

17 (*a*) L. Yuan, W. Lin, S. Zhao, W. Gao, B. Chen, L. He and S. Zhu, *J. Am. Chem. Soc.*, 2012, **134**, 13510–13523; (*b*) H. Chen, W. Lin and L. Yuan, *Org. Biomol. Chem.*, 2013, **11**, 1938–1941; (*c*) J. A. Richard, *Org. Biomol. Chem.*, 2015, **13**, 8169–8172; (*d*) H. Chen, W. Lin, H. Cui and W. Jiang, *Chem.–Eur. J.*, 2015, **21**, 733–745.

18 (*a*) H. Kojima, N. Nakatsubo, K. Kikuchi, S. Kawahara, Y. Kirino, H. Nagoshi, Y. Hirata and T. Nagano, *Anal. Chem.*, 1998, **70**, 2446–2453; (*b*) Y. Gabe, Y. Urano, K. Kikuchi, H. Ko-jima and T. Nagano, *J. Am. Chem. Soc.*, 2004, **126**, 3357–3367; (*c*) E. Sasaki, H. Kojima, H. Nishimatsu, Y. Urano, K. Kikuchi, Y. Hirata and T. Nagano, *J. Am. Chem. Soc.*, 2005, **127**, 3684–3685.

19 (*a*) H. E. Ganther, *Biochemistry*, 1971, **10**, 4089–4098; (*b*) M. Wallenberg, E. Olm, C. Hebert, M. Björnstedt and A. P. Fernandes, *Biochem. J.*, 2010, **429**, 85–93; (*c*) S. J. Fairweather-Tait, Y. Bao, M. R. Broadley, R. Collings, D. Ford, J. E. Hesketh and R. Hurst, *Antioxid. Redox Signaling*, 2011, **14**, 1337–1383; (*d*) M. Björnstedt, S. Kumar and A. Holmgren, *J. Biol. Chem.*, 1992, **267**, 8030–8034; (*e*) S. Kumar, M. Björnstedt and A. Holmgren, *Eur. J. Biochem.*, 1992, **207**, 435–439; (*f*) M. Björnstedt, M. Hamberg, S. Kumar, J. Xue and A. Holmgren, *J. Biol. Chem.*, 1995, **270**, 11761–11764.

20 L. Yan and J. E. Spallholz, *Biochem. Pharmacol.*, 1993, **45**, 429–437.

21 (*a*) N. Karton-Lifshin, E. Segal, L. Omer, M. Portnoy, R. Satchi-Fainaro and D. Shabat, *J. Am. Chem. Soc.*, 2011, **133**, 10960–10965; (*b*) X. Pan, X. Wang, L. Wang, K. Xu, F. Kong and B. Tang, *Anal. Chem.*, 2015, **87**, 7092–7097.

22 (*a*) P. Vaupel, F. Kallinowski and P. Okunieff, *Cancer Res.*, 1989, **49**, 6449–6465; (*b*) H. Harada, *Nat. Commun.*, 2012, **3**, 783; (*c*) D. Hanahan and R. A. Weinberg, *Cell*, 2000, **100**, 57–70; (*d*) M. C. Hung, G. B. Mills and D. Yu, *Nat. Med.*, 2009, **15**, 246–247.

23 (*a*) N. S. Rajasekaran, P. Connell, E. S. Christians, L.-J. Yan, R. P. Taylor, A. Orosz, X.-Q. Zhang, T. J. Stevenson, R. M. Peshock, J. A. Leopold, W. H. Barry, J. Loscalzo, S. J. Odelberg and I. J. Benjamin, *Cell*, 2007, **130**, 427–439; (*b*) V. M. Labunskyy, B. C. Lee, D. E. Handy, J. Loscalzo, D. L. Hat-field and V. N. Gladyshev, *Antioxid. Redox Signaling*, 2011, **14**, 2327–2336.

24 (*a*) C. Mealli, S. Midollini and L. Sacconi, *Inorg. Chem.*, 1978, **17**, 632–637; (*b*) V. V. Matylitsky, A. Shavel, N. Gaponik, A. Eychmüller and J. Wachtveitl, *J. Phys. Chem. C*, 2008, **112**, 2703–2710.

This journal is © The Royal Society of Chemistry 2016